CHEMMEDCHEM

CHEMISTRY ENABLING DRUG DISCOVERY

Accepted Article

Title: Synthesis of 5α,8α-ergosterol peroxide 3-carbamate derivatives and fluorescent mitochondria-targeting conjugate for enhanced anticancer activities

Authors: Ming Bu, Tingting Cao, Hongxia Li, Mingzhou Guo, Burton B. Yang, Chengchu Zeng, and Liming Hu

This manuscript has been accepted after peer review and appears as an Accepted Article online prior to editing, proofing, and formal publication of the final Version of Record (VoR). This work is currently citable by using the Digital Object Identifier (DOI) given below. The VoR will be published online in Early View as soon as possible and may be different to this Accepted Article as a result of editing. Readers should obtain the VoR from the journal website shown below when it is published to ensure accuracy of information. The authors are responsible for the content of this Accepted Article.

To be cited as: *ChemMedChem* 10.1002/cmdc.201700021

Link to VoR: http://dx.doi.org/10.1002/cmdc.201700021

A Journal of

ChemPubSoc Europe

WILEY-VCH

www.chemmedchem.org

Synthesis of 5α,8α-ergosterol peroxide 3-carbamate derivatives and fluorescent mitochondria-targeting conjugate for enhanced anticancer activities

Ming Bu,[a] Tingting Cao,[a] Hongxia Li,[a] Mingzhou Guo,[c] Burton B. Yang,[d] Chengchu Zeng[a] and Liming Hu*[a,b]

Abstract: By inspiration of significant anticancer activity of our previously screened natural ergosterol peroxide (**1**), a series of novel ergosterol peroxide 3-carbamate derivatives were synthesized and characterized. The anti-proliferative activity of synthesized compounds against human hepatocellular carcinoma cells (HepG2, SK-Hep1) and human breast cancer cells (MCF-7, MDA-MB231) were investigated. Compound **3d**, **3f** and their hydrochloride exhibited significant *in vitro* anti-proliferative activity against the tested tumor cell lines, with IC_{50} values ranging from 0.85 to 4.62 μM. Furthermore, fluorescence mitochondria-targeting images showed that the designed coumarin-**3d** conjugate (**5**) localized mainly in mitochondria, leading to enhanced anticancer activities over the parent structure (**1**). As a whole, it appeared that substituent changes to the C-3 position could serve as a promising launch point for further design of this type of steroidal anticancer agents.

Introduction

Endoperoxides (EPOs) are cyclic organic compounds, with an O-O single bond as a peroxidic bridge.[1] EPOs include 1,2-dioxanes, 1,2,4-trioxanes and 1,2,4,5-tetraoxanes, all of which possess the critical peroxide linkage.[2] They play an important role in drug synthesis as well as in medicine,[3] and represent the central part of artemisinin, outstanding antimalarial drugs, honored with the Noble Price in Medicine 2015.[4] Although best known as potent antimalarials,[5] cyclic peroxides also exhibit a range of activities which encompasses antifungal, antiviral and anticancer activity (Figure 1).[6]

Steroidal compounds have drawn attention not only due to unusual and interesting chemical structures, but also due to their widespread application as anti-inflammatory, diuretic, anabolic, contraceptive, and anticancer agents.[7] Most steroidal drugs in use today are semi-synthetic compounds and widely used in traditional medicines by the modification of the steroid ring system and side chains.[8] The interesting structural and stereochemical features of the steroid nucleus provide additional fascination to the researchers, and thereby the introduction of heteroatom, heterocycle, amides or replacement of one or more carbon atoms in the steroidal skeleton has been envisaged to discover new chemical entities with a potential to afford some promising drugs of the future and brings notable modifications of its biological activity.[9]

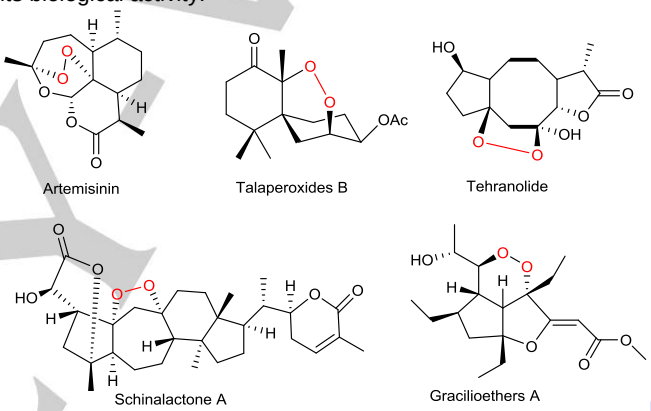

Figure 1. Structures of natural endoperoxides with bioactivities

Among natural EPOs, 1,2-dioxanes are the most frequent constituents of naturally occuring endoperoxides, such as sterol 5α,8α-endoperoxides are the important active lead compounds in drug discovery.[10] Ergosterol peroxide (5α,8α-epidioxiergosta-6,22-dien-3β-ol, EP, **1**) (Figure 2), is a member of a class of fungal secondary metabolites of sterol 5α,8α-endoperoxide derivatives. It can be isolated from many medicinal fungi, such as *Sarcodon aspratus*, *Hericium erinaceum*, *Armillariella mellea*, *lactarius hatsudake*, *hypsizigus marmoreus*, *etc*.[11] Ubiquitous EP (**1**) continues to be isolated from a number of natural sources. A number of biological activities have been attributed to ergosterol peroxide, such as antitumor activity, immunomodulatory activity, inhibitory hemolytic activity, anti-inflammatory activity, and antiviral activity.[12]

In our previous study, we found that **1** purified from *Ganoderma lucidum*, induced cell death and inhibited cell migration, cell cycle progression, and colony growth of human hepatocellular carcinoma cells.[13] We further examined the mechanism associated with this effect and found that treatment with **1** increased expression of Foxo3a mRNA and protein in HepG2 cells. The levels of Puma and Bax, pro-apoptotic proteins, were effectively enhanced. Our results suggest that **1** stimulated Foxo3 activity by inhibiting pAKT and c-Myc and

[a] *M. Bu, T. T. Cao, H.X. Li, Prof. Dr. C. C. Zeng, Prof. Dr. L. M. Hu*
College of Life Science and Bioengineering
Beijing University of Technology
Beijing, 100124, China
E-mail: huliming@bjut.edu.cn
[b] *Prof. Dr. L. M. Hu*
Beijing Key Laboratory of Environmental and Viral Oncology
Beijing University of Technology
Beijing, 100124, China
[c] *Prof. Dr. M. Z. Guo*
Chinese PLA General Hospital,
Beijing, 100853, China
[d] *Prof. Dr. B. B. Yang*
Institute of Medical Science
University of Toronto
Toronto, M4N3M5, Canada

Supporting information for this article is given via a link at the end of the document.

This article is protected by copyright. All rights reserved.

Accepted Manuscript

activating pro-apoptotic protein Puma and Bax to induce cancer cell death. With further clinical development, **1** represents a promising new reagent that can overcome the drug-resistance of tumor cells.[14] Since the amount of purified **1** is not sufficiently to perform *in vivo* experiments and clinical application, we developed approach to synthesize **1** chemically. The synthesis of **1** achieved by the reaction of ergosterol with singlet oxygen ($^1O_2$), which can be conveniently generated photochemically from molecular oxygen (photooxygenation).[15]

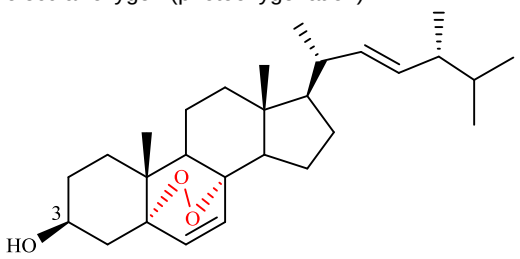

Figure 2. The structure of ergosterol peroxide (EP, **1**).

Acknowledging the limited structure-activity relationship studies for **1**, it is obvious that structurally simpler polar substituent could be advantageously grafted on C-3 position of **1** to increase anticancer activity while simultaneously increasing solubility. *N*-Heterocycles are found in a variety of biologically active compounds and are easily to form water-soluble salts with organic or inorganic acids.[16] It is also noticeable that most of the drugs used in medicine behave as weak acid or base in solution. *N*-Heterocycles drugs with a lone pair of electrons on nitrogen available for protonation are recognized as basic drugs.[17] On the basis of the above details, we designed and synthesized a series of ergosterol peroxide 3-carbamate derivatives. Meanwhile, their biological activities (IC_{50} values) were compared using a MTT assay with four human cancer cell lines. We hope to get valuable information for further design of novel steroidal anticancer agents.

Mitochondria-targeting theranostic probes that enable the simultaneously reporting of and triggering of mitochondrial dysfunctions in cancer cells are highly attractive for cancer diagnosis and therapy.[18] Herein, we also designed the fluorescent mitochondria-targeting theranostic probe through the conjugation of synthesized derivatives with a coumarin-3-carboxylic acid fluorophore.[19] We postulated that the fluorescent conjugates as mitochondria targeting theranostic probes could efficiently leading to enhance anticancer activities.[20]

Results and Discussion

Chemistry

Using natural and commercially available ergosterol as the starting material, we performed chemical synthesis and purification of **1** as described in our previous work.[14] The X-ray crystal structure of **1** was obtained the first time and presented in Figure 3. The derivatives **3a-3j** were synthesized from **1** by the method as shown in Scheme 1. In the first step, **1** was reacted with 4-nitrophenyl chloroformate in DCM using pyridine as the base to obtain intermediate **2**. Then, **2** reacted with different amines in the presence of Et_3N to obtain the desired products **3a-3j**. The courses of reactions were monitored by thin layer chromatography (TLC) plates and/or by staining with H_2SO_4-ethanol solution (5% H_2SO_4 in ethanol). The chemical structures of the compounds synthesized were elucidated on the basis of ^1H NMR, ^{13}C NMR, MS and X-ray. The detailed physical and analytical data are given in experimental part. As shown in Table 1, although asymmetric diamine was used as substrate (Table 1, entry 6), the compound mentioned in Table 1 was the main product.

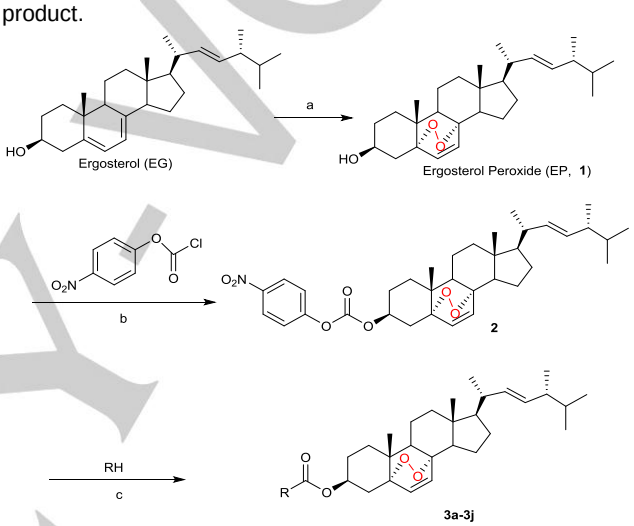

Scheme 1. Synthesis of EP 3-carbamate analogues **3a**-**3j**. Reagents and conditions: (a) O_2, eosine, pyridine, *hv*, 0 °C, 0.5 h; (b) 4-nitrophenyl chloroformate, DCM, pyridine, RT; (c) different amines, Et_3N, DCM, RT.

X-ray crystal structure of **1** was obtained and is presented in Figure 3. The structure confirms the α-stereochemistry of the peroxy bond at C-5 and C-8 positions. Crystallographic data for **1** has been deposited at the Cambridge Crystallographic Data Center with CCDC numbers 1442028.

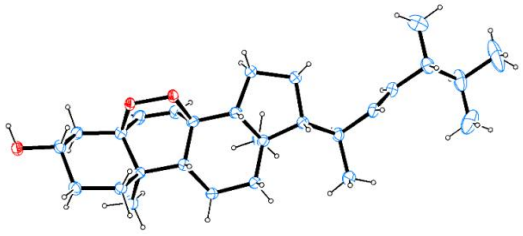

Figure 3. X-ray crystal structure of **1**.

Here a plausible reaction mechanism for the formation of 5α,8α-peroxy moiety from ergosterol is depicted. First, singlet oxygen is generated from sensitization by eosine. Then, the

This article is protected by copyright. All rights reserved.

clear regionselectivity of the singlet oxygen attacks to the C-5 and C-8 positions of the conjugated double bond system in the [4+2] cycloaddition manner. What's more, the α-π-facial stereo-selectivity of the reaction of singlet oxygen with $\triangle^{5,7}$-diene is well accepted owing to the fact that the methyl group at C-10 is β (axial).[21]

Table 1. Ergosterol peroxide 3-carbamate derivatives **3a-3j**.

Entry	Compound	R	Yield (%) [a]
1	**3a**	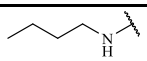	85
2	**3b**	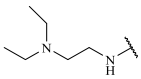	56
3	**3c**	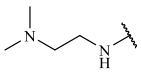	62
4	**3d**	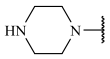	60
5	**3e**	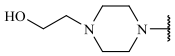	69
6	**3f**	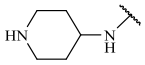	66
7	**3g**	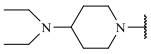	82
8	**3h**	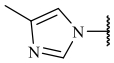	85
9	**3i**	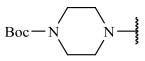	80
10	**3j**	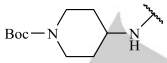	77

[a] Isolated yields.

X-ray crystal structure of **3c** was obtained and is presented in Figure 4. The structure confirms the carbamate structure at C-3 position. Crystallographic data for **3c** has been deposited with CCDC numbers 1514530.

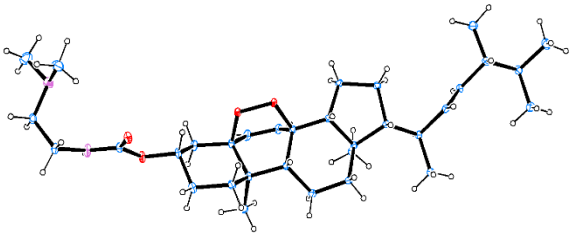

Figure 4. X-ray crystal structure of **3c**.

Biological evaluation

The newly synthesized compounds **3a-3j**, **3d·HCl**, **3f·HCl** and **1** were evaluated for their anti-proliferative activities against human cancer cell lines derived from various human cancer types, including human hepatocellular carcinoma cell lines HepG2, SK-Hep1 and human breast cancer cell lines MDA-MB231, MCF-7. *In vitro* cell-based evaluation of the anti-proliferative activities of the synthesized compounds was carried out using MTT assay. Cisplatin was employed as the positive control. The anticancer potency of the compounds was indicated by IC_{50} values. The results were summarized in Table 2.

Table 2. The anti-proliferative activities of compounds.

Compound	IC_{50} (μM) [a]			
	HepG2	SK-Hep1	MCF-7	MDA-MB231
3a	>40	>40	>40	>40
3b	9.76±0.37	8.21±0.04	11.27±0.06	8.79±0.40
3c	13.60±0.88	10.23±0.32	17.70±0.67	14.55±0.36
3d	0.85±0.06	1.75±0.29	3.26±0.11	4.12±0.38
3d·HCl	0.79±0.12	1.78±0.08	4.00±0.21	3.24±0.14
3e	19.52±0.47	15.23±0.16	12.24±0.35	16.08±0.53
3f	2.83±0.11	0.92±0.04	4.62±0.28	3.99±0.20
3f·HCl	1.96±0.17	0.87±0.07	3.78±0.20	3.27±0.09
3g	29.41±0.61	20.66±0.24	>40	33.05±0.49
3h	>40	>40	>40	>40
3i	24.25±0.23	20.34±0.33	>40	29.87±0.35
3j	22.62±0.18	21.45±0.17	30.80±0.41	>40
1	23.50±0.43	19.71±0.49	26.06±0.18	24.75±0.26
Cisplatin	<0.50	2.39±0.14	6.63±0.27	5.50±0.45

[a] Each data point and error represents the mean ± SD of three experiment results.

The IC_{50} values presented in Table 2 indicate that as compared to the parent **1**, most of the carbamate derivatives (**3a-3j**) possess strong growth inhibition activity against all the four tested adherent cancer cell lines. The screening results suggested a rough SAR: among the nitrogen-contained carbocycle carbamates, the piperazinyl, and piperidinyl moieties were effective in increasing cytotoxicity. Compounds **3d** and **3f** contained piperazinyl and piperidinyl moieties displayed the most significant anti-proliferative activity with the IC_{50} values of 0.85-4.62 μM, which were between 6- and 28-fold more potent than **1**. The compounds with N-methyl, N-ethyl and hydroxyl substituents (**3b**, **3c**, **3e**, and **3g**) at the nitrogen-contained carbocycle demonstrated lower activities. The results also showed that both **3d·HCl** and **3f·HCl** displayed strong anti-

For internal use, please do not delete. Submitted_Manuscript

This article is protected by copyright. All rights reserved.

proliferative activity, therefor, **3d**, **3d·HCl**, **3f** and **3f·HCl** were chosen for further solubility studies. We further analyzed the impact of substituents at 4'-nitrogen atom in piperidine and piperazine ring on cytotoxicities. Compared with **3d** and **3f**, we observed that incorporation of Boc-group on **3i** and **3j** resulted in a significant loss of potency against four cell lines (IC_{50} > 20 μM). The results clearly indicated that 4'-NH was favorable to their cytotoxic activity.

Compounds **3b**, **3d**, **3d·HCl**, **3f**, **3f·HCl** and **1** with good anti-proliferative activities against cancer cells were selected for further *in vitro* cytotoxic evaluation using a non-cancer cell line 293T (human kidney epithelial cell line) as a control. Exponentially growing 293T cells were treated with the compounds at different concentrations for 48 h. Cell-growth inhibition was analyzed by the MTT assay. The results are summarized in Table 3. As shown in Table 3, the median cytotoxic concentration (CC_{50}) showed that most of the tested compounds displayed relative lower cytotoxicity *in vitro* against 293T cells. They exhibited appropriate selectivity between cancer cell line and non-cancer cell line.

Table 3. Cytotoxic activity data against 293T cell lines.

Compound	CC_{50} (μM) [a]
	293T
1	56.82±0.48
3b	61.62±0.79
3d	36.49±0.40
3d·HCl	32.50±0.33
3f	23.48±0.65
3f·HCl	25.86±0.42
Cisplatin	24.22±0.16

[a] Each data point and error represents the mean ± standard deviation of three experiment results.

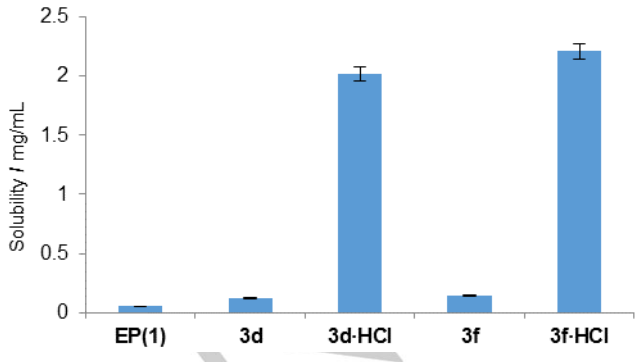

Figure 5. The water solubility of **1**, **3d**, **3d•HCl**, **3f** and **3f•HCl**. Error bars, SD (*n* = 3).

Among derivatives **3a-3j**, piperazinyl (**3d**) and piperidinyl (**3f**) are two of the distinctive *N*-heterocycles those are readily available for protonation in solution and provide opportunity to design new drug structures. The water solubility of **1**, **3d**, **3d·HCl**, **3f** and **3f·HCl** were tested, and the solubilities were 0.05, 0.12, 2.00, 0.15 and 2.20 mg/mL, respectively. The results indicated that the solubility of **3d·HCl** and **3f·HCl** were about 40 times greater than that of **1** (Figure 5).

HepG2 cells were treated with different concentrations of **3f** as indicated for 48 h. Cells were fixed with cold methanol for 15 min and stained with the Diff-Quik-Stain kit, followed by microscopic examination. Typical photos of cell death are shown in Figure 6. HepG2 cells were also treated with **3f** at the concentration of 1 μM for 24 h. Cells were fixed with cold methanol for 15 min and stained with the Diff-Quik-Stain kit, followed by microscopic examination. Careful examination of the cells treated with **3f** revealed the typical vacuoles (Figure 6B). The phenomenon shown that cellular structure integrity has been destroyed by **3f**, such accelerated the cancer cell apoptosis.

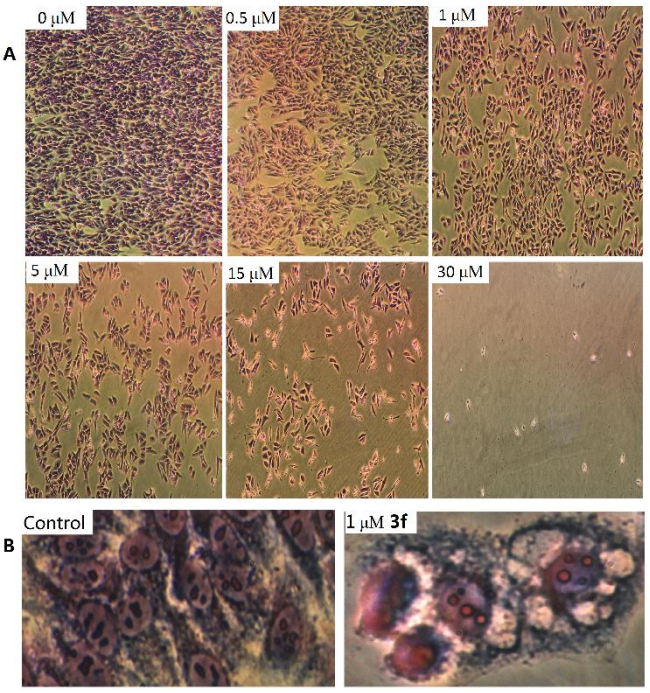

Figure 6. 3f induced cell death of HepG2. (A)Typical photos of cell death were shown. (B) The cells treated with **3f** revealed the typical vacuoles

Epithelial cell migration is a regulated and harmonized mechanism in the cancer cells. It requires their chemotactic migration which is further guided by the protrusive activity of the cellular membrane. Conventional scratch wound motility assay exhibited the ability of **3f** to modulate the migration of HepG2 cells in a denuded area. Cell migration was monitored using scratch assay. Typical photos of cell motility are shown in Figure 7A. It was found that **3f**-treated HepG2 cells displayed lower speeds of motility than the control cells, thereby indicating the inhibition of proliferation of HepG2 cells by **3f** (Figure 7B).

Accepted Manuscript

This article is protected by copyright. All rights reserved.

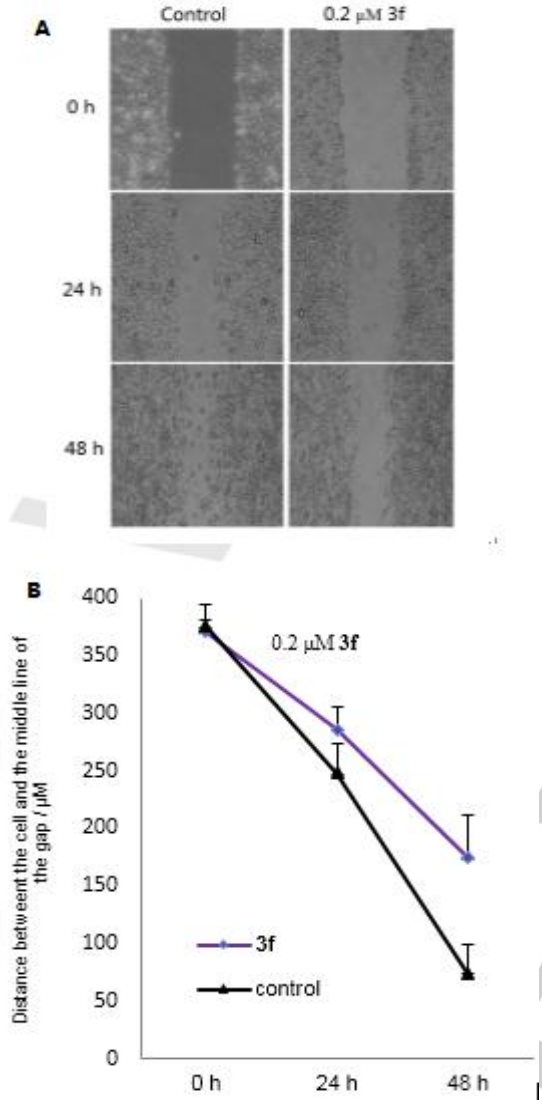

Figure 7. Cell motility studies with compound **3f**. (A) Typical photos of cell motility were shown. (B) Migration rates were measured and calculated. Error bars, SD (n = 3).

Fluorescent mitochondria-targeting probe

Based on significant anticancer activity of **3d**, we designed a fluorescent mitochondria-targeting probe coumarin-**3d** (**5**) through the conjugation of **3d** with a coumarin-3-carboxamide fluorophore. Designed conjugate probe **5** was synthesized *via* the routes outlined in Scheme 2.

With the probe **5** in hand, we first investigated its optical properties (Figure 8). In general, it possess typical optical properties of the courmarin-3-carboxamide fluorophore, with maximum excitation wavelength (λ_{Ex}) of about 469.5 nm and emission wavelength (λ_{Em}) of about 404 nm. The large Stokes shift of probe 65.5 nm ensured good photophysical properties for fluorescence imaging studies in living cells.

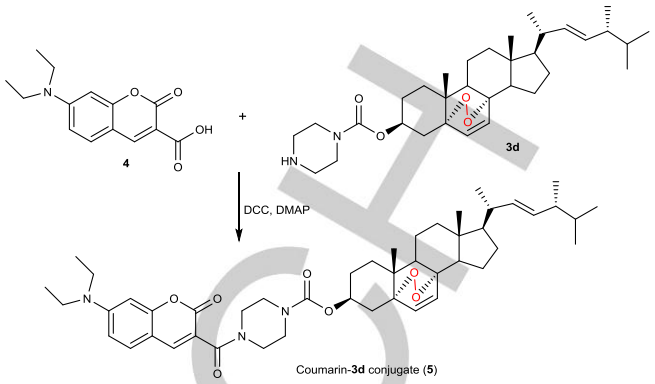

Scheme 2. Synthetic of the probe coumarin-**3d** (**5**). Reagents and conditions: DCC, DMAP, DCM, RT, 36 h.

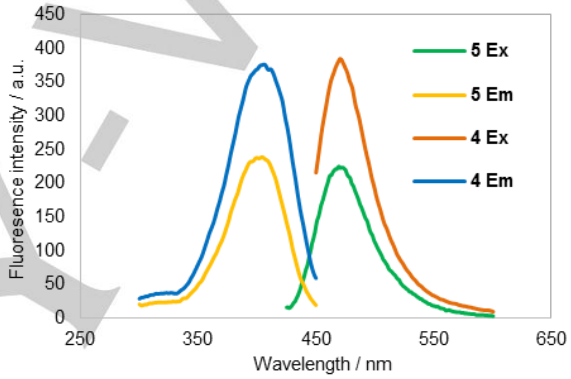

Figure 8. Fluorescence excitation spectra and emission spectra for probes **4** and **5** (1.0 μM in DMSO).

We next examined the subcellular localization of the designed conjugates **5** in living human liver cancer cells (HepG2 and MCF-7) with the commercially available mitochondria-specific green dye Rhodamine 123 (Rh123) (λ_{Ex} = 488 nm and λ_{Em} = 515-530 nm). The intracellular fluoroscope imaging was explored on a 710M confocal laser scanning microscopy (Carl Zeiss, Germany). As shown in Figure 9b, cells were extensively stained by **5** (5 μM) after 2 h of incubation, and strong blue fluorescence was detected inside the cells with excitation at λ = 430-500 nm, which indicated good cell membrane permeability and high cellular uptake of **5**. The subcellular localization study showed that compound **5** could colocalize strongly with Rh123 in mitochondria, with an extensive blue-green colour in the merged fluorescence images of **5** and Rh123 (Figure 9d).

Having proved mitochondrial localization of our designed conjugate **5**, we then measured the anti-proliferative activities of **5** against four selected human cancer cell lines (HepG2, Sk-Hep1 MCF-7 and MDA-MB231). The results in Table 4 show that designed coumarin-**3d** (**5**) conjugate localized mainly in mitochondria, leading to enhanced anticancer activities over ergosterol peroxide (**1**), but lower than **3d**. We therefore postulated that, upon cell uptake, the mitochondria-targeting **5** could efficiently trigger the compound localized in mitochondria,

For internal use, please do not delete. Submitted_Manuscript

This article is protected by copyright. All rights reserved.

in which subsequent triggering of mitochondrial dysfunctions in cancer cells and induce cell apoptosis

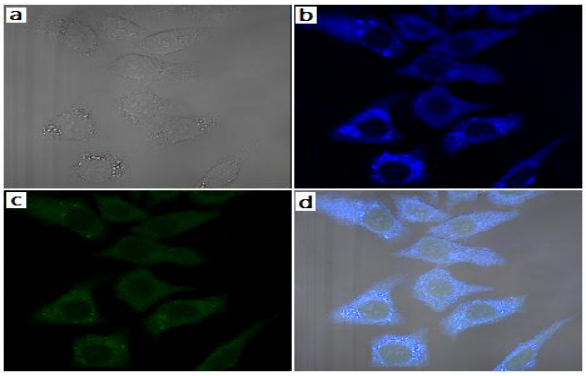

Figure 9. Confocal laser scanning microscopic images of HepG2 cells treated with **5** (5 μM, 2 h) in the presence of Rh123 (0.5 μM, 20 min) in PBS buffer. a) Cell images in bright field. b) Fluorescence images of HepG2 cells stained with **5**. c) Fluorescence images of cells stained with Rh123. d) Merged images of b) and c).

Table 4. The anti-proliferative activities of compounds.

Compound	IC_{50} (μM) [a]			
	HepG2	SK-Hep1	MCF-7	MDA-MB231
4	>100	>100	>100	>100
5	7.86±0.49	9.54±0.62	10.46±0.36	8.28±0.52

[a] Each data point and error represents the mean ± standard deviation of three experiment results.

We further analyzed the impact of substituents at 4'-nitrogen atom in piperazine ring on anti-proliferative activities. Compared with **3d** and probe **5**, we observed that incorporation of coumarin-3-carboxylic acid on **3d** resulted in a loss of potency against four cell lines. The results further indicated that 4'-NH of **3d** was the essential to the cytotoxic activity. In contrast, much weaker anti-proliferative activities were measured for **4** and **1**, which suggested that the anti-proliferative activities of compound **5** was associated with the synergistic effect of these two components. Even so, this study highlights the potential of using mitochondria-targeting fluorophore to directly visualize subcellular drug delivery in living cells.

Conclusions

In summary, a series of novel ergosterol peroxide 3-carbamate derivatives from ergosterol by a three-step reaction route were synthesized and evaluated for their anticancer activities. Preliminary structure-activity relationships were put forward based on the biological results. Some of the synthesized compounds exhibited potent anticancer activities against the four tested cancer cell lines *in vitro*. In particular, compound **3d**, **3f**, **3d·HCl** and **3f·HCl** were the most promising derivatives, with IC_{50} values ranging from 0.85-4.62 μM against all the four cancer cell lines. Among them, the solubility of **3d·HCl** and **3f·HCl** was about 40 times greater than that of **1**. In an overall view, the 5α,8α-ergosterol peroxide 3-carbamate derivatives will provide better insight into the effect of the C-3 site on anticancer activity for designing potential steroidal endoperoxide anticancer agents. What's more, fluorescence images showed that the designed coumarin-**3d** (**5**) conjugate localized mainly in mitochondria, leading to enhanced anticancer activities over the parent structure **1**. This study highlights the potential of using mitochondria-targeting fluorophore to directly visualize subcellular drug delivery in living cells. Future work will also focus on the synthesis of additional candidate structures with different substituents to address specific cancer cell lines. It appeared that substituent changes to the steroidal C-3 position could serve as a promising launch point for further design of this type of steroidal anticancer agents.

Experimental Section

Chemistry

All commercially available reagents were used without further purification Melting points (uncorrected) were determined on a MP120 auto point apparatus (Hanon instruments Corp., Jinan, China). The ^{1}H NMR and ^{13}C NMR spectra were measured on a Bruker Avance DRX400 spectrometer with TMS and solvent signals allotted as internal standards. The chemical shifts of the ^{1}H NMR and ^{13}C NMR were expressed in ppm (*δ*). ESI mass spectra were obtained on an Esquire 6000 Mass Spectrometer. X-ray diffraction data were collected on *CrysAlis PRO*, Agilent Technologies. Silica gel (300-400 mesh) was used for analytical and flash chromatography. DCM refers to dichloromethane, Et_3N refers to triethylamine, and RT refers to room temperature.

Ergosterol peroxide (1).[14] White needles; m.p. 181.5-183 °C. ^{1}H NMR (400 MHz, $CDCl_3$) *δ* (ppm) 0.82 (d, *J* = 6.8 Hz, 3H), 0.83 (s, 3H), 0.84 (d, *J* = 6.8 Hz, 3H), 0.89(s, 3H), 0.91 (d, *J* = 6.9 Hz, 3H), 1.00 (d, *J* = 6.4 Hz, 3H), 3.97 (m, 1H), 5.12 (dd, *J* = 8.0, 15.2 Hz, 1H), 5.23 (dd, *J* = 7.6, 15.2 Hz, 1H), 6.24 (d, *J* = 8.4 Hz, 1H), 6.51 (d, *J* = 8.4 Hz, 1H). ^{13}C NMR (100 MHz, $CDCl_3$) *δ* (ppm) 12.9, 17.6, 18.2, 19.6, 19.9, 20.6, 20.9, 23.4, 28.6, 30.1, 33.1, 34.7, 37.0, 37.0, 39.3, 39.7, 42.8, 44.6, 51.1, 51.7, 56.2, 66.4, 79.4, 82.2, 130.7, 132.3, 135.2, 135.4. ESI-MS *m/z*: 451.4 $[M+Na]^+$, 467.3 $[M+K]^+$.

General procedure for the synthesis of compounds 3a-3j. To a stirred solution of **1** (100 mg, 0.28 mmol) and 4-nitrophenyl chloroformate (129 mg, 0.64 mmol, 2.3 eq) in anhydrous DCM (2 mL) at room temperature under nitrogen gas was added pyridine (50 mg, 0.64 mmol, 2.3 eq), and stirring continued for 2 h. After completion (by TLC), DCM (10 mL), and H_2O (10 mL) were added. The organic phase was separated, washed with aq. Na_2CO_3, and brine, dried over Na_2SO_4, and concentrated in vacuo to afford yellow residue **2**. To a solution of the residue in DCM (2.5 mL) was added amine (3 eq) and Et_3N (3 eq), and stirring continued at room temperature for 2 h. After completion (by TLC), DCM (15 mL) and H_2O (15 mL) were added. The organic phase was separated, washed with aq. Na_2CO_3 and brine, dried over Na_2SO_4, and concentrated in vacuo to give yellow residue, and the residue was

This article is protected by copyright. All rights reserved.

subjected to chromatographic separation on silica gel with petroleum ether/acetone/triethylamine.

5α,8α-epidioxyergosta-3-yl-butylcarbamate(3a). White solid, m.p. 165.9-167.4°C; ^{1}H NMR (400 MHz, $CDCl_3$) δ 6.50 (d, J = 8.5 Hz, 1H), 6.22 (d, J = 8.5 Hz, 1H), 5.18 (d, J = 15.3, 7.7 Hz, 2H), 4.94-4.81 (m, 1H), 4.54 (s, 1H), 3.22-3.07 (m, 2H), 2.15 (dd, J = 13.1, 4.0 Hz, 1H), 1.99 (m, 5H), 1.85 (dd, J = 13.0, 6.8 Hz, 1H), 1.75 (d, J = 9.2 Hz, 1H), 1.71-1.64 (m, 2H), 1.63-1.53 (m, 3H), 1.56-1.41 (m, 6H), 1.34 (qd, J = 14.1, 6.9 Hz, 4H), 1.28-1.16 (m, 3H), 0.99 (s, 3H), 0.91 (m, 9H), 0.82 (m, 9H); ^{13}C NMR (100 MHz, $CDCl_3$) δ 155.7, 135.2, 132.3, 130.8, 81.8, 79.3, 69.6, 56.2, 51.6, 51.0, 44.5, 42.8, 39.7, 39.3, 36.9, 34.3, 33.5, 33.1, 32.1, 28.6, 26.7, 23.4, 20.9, 20.6, 19.9, 19.6, 18.1, 17.5, 13.7, 12.9; MS (ESI) *m/z*: 528.8 $[M+H]^+$.

5α,8α-epidioxyergosta-3-yl-(2-(diethylamino)ethyl)carbamate(3b). White solid, m.p. 154.8-156.4 °C; ^{1}H NMR (400 MHz, $CDCl_3$) δ 6.51 (d, J = 8.5 Hz, 1H), 6.24 (d, J = 8.5 Hz, 1H), 5.26-5.17 (m, 2H), 5.14 (d, J = 8.0 Hz, 1H), 4.96-4.82 (m, 1H), 3.25 (d, J = 5.3 Hz, 2H), 2.40 (m, 2H), 2.23 (m, 6H), 2.17 (dd, J = 10.3, 4.1 Hz, 1H), 2.07-1.94 (m, 6H), 1.87 (dd, J = 13.0, 6.8 Hz, 1H), 1.79-1.66 (m, 2H), 1.63-1.46 (m, 6H), 1.44-1.34 (m, 2H), 1.29-1.21 (m, 3H), 1.01 (d, J = 6.6 Hz, 3H), 0.95-0.88 (m, 6H), 0.84 (m, 9H). ^{13}C NMR (100 MHz, $CDCl_3$) δ 155.8, 135.3, 135.2 132.3, 130.8, 81.8, 79.3, 69.6, 58.2, 56.2, 51.6, 51.0, 45.1, 44.5, 42.8, 39.7, 39.3, 38.2, 36.9, 34.3, 33.5, 33.1, 28.6, 26.7, 23.3, 20.9, 20.6, 19.9, 19.6, 18.1, 17.5, 12.9; MS (ESI) *m/z*: 571.5 $[M+H]^+$.

5α,8α-epidioxyergosta-3-yl-(2-(dimethylamino)ethyl)carbamate (3c). White solid, m.p. 153.9-155.2 °C; ^{1}H NMR (400 MHz, $CDCl_3$) δ 6.50 (d, J = 8.5 Hz, 1H), 6.22 (d, J = 8.5 Hz, 1H), 5.24-5.12 (m, 2H), 4.90-4.82 (m, 1H), 3.21 (d, J = 5.1 Hz, 2H), 2.59-2.48 (m, 6H), 2.19-2.10 (m, 1H), 1.98 (dd, J = 15.8, 7.5 Hz, 4H), 1.85 (dd, J = 13.0, 6.8 Hz, 1H), 1.77-1.64 (m, 4H), 1.57 (dd, J = 15.2, 5.4 Hz, 2H), 1.52-1.47 (m, 2H), 1.39-1.31 (m, 2H), 1.27-1.19 (m, 5H), 1.01 (m, 9H), 0.93-0.88 (m, 6H), 0.84-0.79 (m, 9H); ^{13}C NMR (100 MHz, $CDCl_3$) δ 155.9, 135.3, 135.2, 132.3, 130.8, 81.8, 79.3, 69.6, 56.2, 51.8, 51.6, 51.0, 46.8, 44.6, 42.8, 39.7, 39.3, 36.9, 34.3, 33.5, 33.1, 28.6, 26.8, 23.4, 20.9, 20.6, 19.9, 19.6, 18.1, 17.6, 12.9, 11.6; MS (ESI) *m/z*: 543.7 $[M+H]^+$.

5α,8α-epidioxyergosta-3-yl-(piperazine-1)carbamate (3d). Yellow solid, m.p. 200.9-202.1 °C; ^{1}H NMR (400 MHz, $CDCl_3$) δ 6.50 (d, J = 8.5 Hz, 1H), 6.23 (d, J = 8.5 Hz, 1H), 5.18 (qd, J = 15.3, 7.7 Hz, 2H), 4.96-4.83 (m, 1H), 3.47-3.39 (m, 4H), 2.83 (s, 4H), 2.20-2.14 (m, 2H), 2.05-1.98 (m, 4H), 1.86-1.81 (m, 1H), 1.78-1.68 (m, 2H), 1.59 (m, 2H), 1.54-1.44 (m, 4H), 1.38 (m, 1H), 1.28-1.19 (m, 4H), 1.00 (d, J = 6.6 Hz, 3H), 0.90 (m, 6H), 0.82 (m, 9H); ^{13}C NMR (100 MHz, $CDCl_3$) δ 154.7, 135.2, 135.1, 132.2, 130.8, 126.2, 125.1, 122.2, 115.7, 81.8, 79.4, 70.5, 56.2, 51.6, 51.0, 45.6, 44.5, 42.8, 39.7, 39.3, 36.9, 34.3, 33.6, 33.1, 28.6, 26.8, 23.4, 20.9, 20.6, 19.9, 19.6, 18.1, 17.5, 12.9; MS (ESI) *m/z*: 541.6$[M+H]^+$.

5α,8α-epidioxyergosta-3-yl-((4-hydroxyethyl)piperazine-1)carbamate (3e). White solid, m.p. 201.5-203.2 °C; ^{1}H NMR (400 MHz, $CDCl_3$) δ 6.51 (d, J = 8.5 Hz, 1H), 6.23 (d, J = 8.5 Hz, 1H), 5.18 (qd, J = 15.3, 7.7 Hz, 2H), 4.95-4.84 (m, 1H), 3.68-3.58 (m, 2H), 3.47 (d, J = 4.4 Hz, 4H), 2.59-2.53 (m, 2H), 2.52-2.41 (m, 4H), 2.22-2.13 (m, 1H), 2.10-1.92 (m, 5H), 1.85 (dd, J = 13.0, 6.8 Hz, 1H), 1.80-1.66 (m, 3H), 1.62-1.43 (m, 6H), 1.41-1.32 (m, 2H), 1.23 (dd, J = 9.7, 5.7 Hz, 3H), 1.00 (d, J = 6.6 Hz, 3H), 0.91 (m, 6H), 0.82 (m, 9H); ^{13}C NMR (100 MHz, $CDCl_3$) δ 154.6, 135.2, 135.1, 132.3, 130.8, 81.8, 79.3, 70.5, 59.4, 57.7, 56.2, 52.6, 51.6, 51.0, 44.5, 42.7, 39.7, 39.3, 36.9, 34.3, 33.6, 33.1, 28.6, 26.8, 23.4, 20.9, 20.6, 19.9, 19.6, 18.1, 17.5, 12.9; MS (ESI) *m/z*: 585.7 $[M+H]^+$.

5α,8α-epidioxyergosta-3-yl-(piperidin-4-methylamine)carbamate (3f). Yellow solid, m.p. 204.4-206.3 °C; ^{1}H NMR (400 MHz, $CDCl_3$) δ 6.50 (d, J = 8.5 Hz, 1H), 6.23 (d, J = 8.5 Hz, 1H), 5.18 (qd, J = 15.3, 7.7 Hz, 2H), 4.93-4.81 (m, 1H), 4.20 (t, J = 15.8 Hz, 1H), 3.03-2.91 (m, 1H), 2.88-2.74 (m, 3H), 2.16 (dd, J = 10.9, 3.3 Hz, 1H), 2.05-1.97 (m, 4H), 1.92 (m, 1H), 1.81 (m, 3H), 1.69 (dd, J = 10.5, 3.5 Hz, 2H), 1.59-1.49 (m, 6H), 1.38 (dd, J = 9.4, 4.9 Hz, 3H), 1.26-1.18 (m, 5H), 1.00 (d, J = 6.6 Hz, 3H), 0.91 (d, J = 6.7 Hz, 6H), 0.82 (m, 9H); ^{13}C NMR (100 MHz, $CDCl_3$) δ 154.7, 135.2, 132.3, 130.8, 125.1, 122.3, 81.8, 79.3, 70.3, 56.2, 51.6, 51.0, 48.7, 48.2, 44.5, 42.8, 42.7, 39.7, 39.3, 36.9, 35.3, 33.1, 28.6, 26.8, 23.3, 20.8, 20.6, 19.9, 19.6, 18.1, 17.5, 12.9; MS (ESI) *m/z*: 555.6 $[M+H]^+$.

5α,8α-epidioxyergosta-3-yl-(4-(diethylamino)piperidine-1)carbamate (3g). White solid, m.p. 158.9-161.8 °C; ^{1}H NMR (400 MHz, $CDCl_3$) δ 6.50 (d, J = 8.5 Hz, 1H), 6.23 (d, J = 8.5 Hz, 1H), 5.18 (qd, J = 15.3, 7.7 Hz, 2H), 4.92-4.82 (m, 1H), 4.14 (d, J = 31.6 Hz, 2H), 2.76-2.62 (m, 3H), 2.55 (q, J = 7.1 Hz, 4H), 2.20-2.11 (m, 1H), 1.99 (td, J = 10.2, 9.8, 5.7 Hz, 4H), 1.85 (m, 1H), 1.78-1.67 (m, 5H), 1.60-1.36 (m, 10H), 1.26-1.20 (m, 3H), 1.06-0.98 (m, 9H), 0.89 (m, 6H), 0.82 (m, 9H); ^{13}C NMR (100 MHz, $CDCl_3$) δ 154.6, 135.3, 135.2, 132.3, 130.8, 81.8, 79.3, 70.2, 58.1, 56.2, 51.6, 51.0, 44.5, 43.6, 43.5, 42.8, 39.7, 39.3, 36.9, 34.3, 33.6, 33.1, 28.6, 26.8, 20.9, 20.6, 19.9, 19.6, 18.1, 17.5, 13.6, 12.9; MS (ESI) *m/z*: 611.6 $[M+H]^+$.

5α,8α-epidioxyergosta-3-yl-((4-methyl)imidazole-1)carbamate(3h). White solid, m.p. 166.4-167.6 °C; ^{1}H NMR (400 MHz, $CDCl_3$) δ 8.01 (s, 1H), 7.10 (s, 1H), 6.55 (d, J = 8.5 Hz, 1H), 6.26 (d, J = 8.5 Hz, 1H), 5.26-5.13 (m, 3H), 2.30 (m, 1H), 2.21 (t, J = 3.1 Hz, 3H), 2.13-2.07 (m, 2H), 2.00 (m, 3H), 1.86 (m, 1H), 1.80-1.74 (m, 2H), 1.65 (m, 2H), 1.59-1.51 (m 3H), 1.49-1.43 (m, 1H), 1.39 (m, 1H), 1.25 (m, 4H), 1.02-0.99 (m, 3H), 0.91 (m, 6H), 0.85-0.81 (m, 9H); ^{13}C NMR (100 MHz, $CDCl_3$) δ 147.7, 136.5, 135.1, 134.6, 132.4, 131.2, 113.1, 81.7, 79.5, 74.1, 56.2, 51.8, 56.2, 51.6, 51.0, 44.6, 42.8, 39.7, 39.2, 36.9, 34.2, 33.1, 33.0, 28.6, 26.2, 23.4, 20.9, 20.6, 19.9, 19.6, 18.1, 17.5, 13.5, 12.9; MS (ESI) *m/z*: 537.7 $[M+H]^+$.

5α,8α-epidioxyergosta-3-yl-((4-*tert*-butyl)piperazine-1)carbamate (3i). White solid, m.p. 208.9-210.4 °C; ^{1}H NMR (400 MHz, $CDCl_3$) δ 6.51 (d, J = 8.5 Hz, 1H), 6.23 (d, J = 8.5 Hz, 1H), 5.18 (m, 2H), 4.95-4.84 (m, 1H), 3.40 (s, 8H), 2.17 (dd, J = 13.7, 4.1 Hz, 1H), 1.99 (m, 5H), 1.85 (m, 1H), 1.73-1.68 (m, 2H), 1.58 (m, 2H), 1.50 (m, 5H), 1.46 (s, 9H), 1.37 (m, 1H), 1.26-1.19 (m, 3H), 1.00 (d, J = 6.6 Hz, 3H), 0.93-0.90 (m, 6H), 0.82 (m, 9H); ^{13}C NMR (100 MHz, $CDCl_3$) δ 154.6, 135.2, 135.1, 132.3, 130.8, 125.1, 122.7, 81.8, 80.5, 80.1, 79.3, 70.7, 56.2, 51.6, 51.0, 44.5, 42.8, 39.7, 39.3, 36.9, 34.3, 33.5, 33.1, 28.6, 28.4, 26.8, 20.9, 20.6, 19.9, 19.6, 18.1, 17.5, 12.9; MS (ESI) *m/z*: 641.8 $[M+H]^+$.

5α,8α-epidioxyergosta-3-yl-((4-tert-butyl)piperidine-1)carbamate(3j). White solid, m.p. 209.3-210.6 °C; ^{1}H NMR (400 MHz, $CDCl_3$) δ 6.51 (d, J = 8.5 Hz, 1H), 6.23 (d, J = 8.5 Hz, 1H), 5.19 (qd, J = 15.3, 7.7 Hz, 2H), 4.88 (s, 1H), 4.49 (s, 1H), 4.00 (s, 2H), 3.63 (s, 1H), 2.85 (t, J = 11.8 Hz, 2H), 2.16 (dd, J = 13.9, 4.4 Hz, 1H), 2.04-1.96 (m, 4H), 1.95-1.87 (m, 3H) 1.85 (m, 1H), 1.69 (m, 3H), 1.55 (m, 6H), 1.46 (s, 9H), 1.38 (m, 1H), 1.26 (m, 6H), 1.01 (d, J = 6.6 Hz, 3H), 0.93-0.88 (m, 6H), 0.84-0.81 (m, 9H); ^{13}C NMR (100 MHz, $CDCl_3$) δ 154.6, 154.7, 135.2, 135.1, 132.3, 130.8, 81.8, 79.6, 79.3, 69.9, 56.2, 51.6, 51.0, 48.2, 44.5, 42.8, 39.7, 39.3, 36.9, 34.3, 33.5, 33.1, 32.4, 28.6, 28.4, 23.4, 20.9, 20.6, 19.9, 19.6, 18.1, 17.6, 12.9; MS (ESI) *m/z*: 555.7 $[M+H]^+$.

Compounds 3d·HCl & 3f·HCl. To a stirred solution of 1% HCl (5 mL) was added compound **3d** or **3f** (1 mmol). The mixture was stirred at RT for 15 min. Then, the precipitate was collected by filtration and washed by cold 50% aq EtOH (5 mL) to afford **3d·HCl** or **3f·HCl**.

Accepted Manuscript

This article is protected by copyright. All rights reserved.

Coumarin-3-carboxylic acid (**4**).[22] A suspension of 4-(diethylamino)-2-hydroxybenzaldehyde (1.00 g, 5.18 mmol, 1.00 equiv), meldrum's acid (0.75 g, 5.18 mmol, 1.00 equiv), piperidine (0.04 g, 0.52 mmol, 0.10 equiv) and two drops of acetic acid in ethanol (abs, 8 mL) was stirred for 30 min at room temperature and heated to reflux for 3 h. The reaction mixture was concentrated in vacuum and poured on 15 mL of ice water. The resulting precipitate was collected and washed with ethanol to give 854 mg (63%) of an orange crystalline solid. ^{1}H NMR (400 MHz, $CDCl_3$) δ 12.50 (br s, 1H, –COOH), 8.58 (s, 1H, CH=C), 7.63 (d, 1H, J= 9.0 Hz, 5H-ph), 6.79 (d, 1H, *J*= 9.0 Hz, 6H-ph), 6.57 (s, 1H, 8H-ph), 3.48 (q, 4H, *J* = 7.0 Hz, $N(C\underline{H}_2–CH_3)_2$), 1.14 (t, 6H, *J* = 6.9 Hz, $N(CH_2–C\underline{H}_3)_2$). ^{13}C NMR (100 MHz, $CDCl_3$) δ 165.5, 164.5, 158.1, 153.8, 150.2, 132.0, 110.0, 108.5, 105.5, 96.8, 77.4, 77.1, 76.7, 45.3, 12.4. MS (ESI) *m/z*: 260.0 $[M-H]^-$.

Synthesis of compound 5. Coumarin-3-carboxylic acid **4** (44 mg, 0.15 mmol, 13 equiv), DCC (31 mg, 0.15 mmol, 13 equiv), and DMAP (2.0 g, 10%) were added to a solution of **3d** (54 mg, 0.1 mmol, 1.0 equiv) in anhydrous DCM (15 mL). The reaction mixture was stirred at RT for 36 h and filtrated. The filtrate was removed under vacuum, and was purified by flash column chromatography to provide **5** (32 mg). Yellow crystals. ^{1}H NMR (400 MHz, $CDCl_3$) δ 7.87 (s, 1H), 7.30 (d, *J* = 8.9 Hz, 1H), 6.60 (dd, J = 8.9, 2.3 Hz, 1H), 6.49 (dd, *J* = 11.9, 5.3 Hz, 2H), 6.23 (d, J = 8.5 Hz, 1H), 5.18 (qd, *J* = 15.3, 7.7 Hz, 2H), 4.97-4.85 (m, 1H), 3.72 (s, 2H), 3.54 (s, 4H), 3.44 (q, *J* = 7.1 Hz, 4H), 3.38 (s, 2H), 2.17 (d, J = 4.8 Hz, 1H), 2.03 (dd, *J* = 16.1, 8.3 Hz, 4H), 1.85 (d, J = 6.5 Hz, 1H), 1.75-1.70 (m, 1H), 1.63 (m, 4H), 1.58 (dd, *J* = 14.9, 5.6 Hz, 2H), 1.51 (t, J = 5.8 Hz, 2H), 1.40-1.36 (m, 1H), 1.25 (d, *J* = 4.8 Hz, 4H), 1.23 (m, 6H), 1.01 (m, 3H), 0.90 (m, 6H), 0.82 (m, 9H). ^{13}C NMR (100 MHz, $CDCl_3$) δ 165.2, 159.1, 157.3, 154.5, 151.8, 135.2, 135.1, 132.3, 130.8, 129.9, 115.8, 109.4, 107.7, 96.9, 81.8, 79.3, 70.8, 56.2, 51.6, 51.0, 44.9, 44.5, 42.7, 39.7, 39.3, 36.9, 34.3, 33.5, 33.0, 28.6, 23.3, 20.9, 19.9, 19.6, 18.1, 17.5, 12.8, 12.4.

Biology

Cell proliferative assay. The effect of derivatives on cell proliferation was evaluated by MTT (3-(4,5-dimethylthiazol-2-yl)-2,5-diphenyltetrazolium bromide assay. Human hepatic carcinoma cells (HepG2, SK-Hep1) and human breast cancer cells (MCF-7, MDA-MB231) were used in the study. The cells were cultured in DMEM/RPMI1640 supplemented with 10% FBS, 100 U/mL penicillin/streptomycin at 37 °C in an incubator containing 5% CO_2. Cells (1×10^4 cells/mL) were seeded into 96-well plates and were incubated at 37 °C overnight in a humidified incubator containing 5% CO_2. Cells were dosed with compounds at final concentrations ranging from 0.2 μM to 40 μM in each well of the plates. The cells were incubated for various periods and analyzed by MTT assay to analyze rates of cell proliferation as described. Cell survival was determined by measuring the absorbance at 490 nm using a microplate reader. A calibration curve was prepared using the SPSS to determine the IC_{50} of the target compounds. Cytotoxicity as IC_{50} for each cell line is the concentration of compound which reduced by 50% the optical density of treated cells (48 h) with respect to untreated cells using the MTT assay.

Cell migration assay. Migration assay was performed by wound scratch test. Briefly, 3×10^5 cells were seeded in each well of 6-well plates and incubated overnight. The cells were scratched using 20 μL pipette tips. The cultures were washed with PBS to remove cell debris. Compound **3f** was added to the cultures at a concentration of 0.2 μM. Cellular motility was monitored and photographed. Microscope images of the scratched cultures were captured at the beginning and at different intervals later. Distance travelled from the initial scratch site was measured and the migration distance was quantified.

Living cell staining for subcellular localization. HepG2 cell lines were grown on glass cover-slips in 6-well plate (0.4 million cells in 2 mL of medium per well). For colocalization in mitochondria, the cells were incubated with **5** (5 μM) for 30 min at 37 °C and mitochondria-specific green dye Rh123 (100 nM) was added in the last 10 min of incubation. After removal of HBSS buffer and three times of wash with PBS, the cells were fixed with 4% para-formaldehyde for 15 min, and then washed with PBS for three times. The cover-slips were sealed with paraffin for image.

Confocal microscopic imaging. Confocal images were captured with a 710M confocal microscope (Carl Zeiss, Germany), original magnification 100×. 520 nm was used for excitation of Rh123. For compound **5**, the excitation laser was 405-410 nm and images were collected at emission of 465-470 nm. After image acquisition, colocalization analysis of compound **5** and the Mito specific dyes on images were processed by using LSM 510 software.

Acknowledgements

The authors would like to acknowledge financial support from the Chinese Natural Science Foundation Project (21272020), Beijing Key Laboratory of Environmental and Viral Oncology and Beijing Key Laboratory for Green Catalysis and Separation.

Keywords: ergosterol peroxide • carbamate • fluorescence image• coumarin • mitochondria-targeting

[1] M. Bauch, M. Klaper, T. Linker, *J. Phys. Org. Chem.* **2016**. DOI: 10.1002/poc.3607.

[2] I. Fernandez, A. Robert, *Org. Biomol. Chem.* **2011**, *9*, 4098-4107.

[3] a) P. Pozarowski, D. H. Halicka, Z. Darzynkiewicz, *Cell Cycle* **2003**, *2*, 377-383; b) M. Axelrod, V. L. Gordon, M. Conaway, A. Tarcsafalvi, D. J. Neitzke, D. Gioeli, M. J. Weber, *Oncotarget* **2013**, *4*, 622-635.

[4] E. Callaway, D. Cyranoski, *Nature* 2015, *526*, 174-175.

[5] R. K. Haynes, K. W. Cheu, D. N'Da, P. Coghi, D. Monti, *Infect. Disord.: Drug Targets* **2013**, *13*, 217-277.

[6] a) M. Jung, H. Kim, K. Lee, M. Park, *Mini-Rev. Med. Chem.* **2003**, *3*, 159-165; b) M. Jung, H. Kim, K. Lee, M. Park, *Mini-Rev. Med. Chem.* **2003**, *3*, 159-165; c) Y. Imamura, M. Yukawa, M. Ueno, K. i. Kimura, E. Tsuchiya, *FEBS J.* **2014**, *281*, 4612-4621; d) H. Li, H. Huang, C. Shao, H. Huang, J. Jiang, X. Zhu, Y. Liu, L. Liu, Y. Lu, M. Li, Y. Lin, Z. She, *J. Nat. Prod.* **2011**, *74*, 1230-1235; e) S. Noori, Z. M. Hassan, *Tumor Biol.* **2014**, *35*, 257-264; f) S. M. N. Efange, R. Brun, S. Wittlin, J. D. Connolly, T. R. Hoye, T. McAkam, F. L. Makolo, J. A. Mbah, D. P. Nelson, K. D. Nyongbela, C. K. Wirmum, *J. Nat. Prod.* **2009**, *72*, 280-283; g) F. He, J. X. Pu, S. X. Huang, Y. Y. Wang, W. L. Xiao, L. M. Li, J P. Liu, H. B. Zhang, Y. Li, H. D. Sun, *Org. Lett.* **2010,** 12, 1208-1211.

[7] a) J. R. Hanson, *Nat. Prod. Rep.* **2010**, *27*, 887-899; b) L. H. Shan, H. M. Liu, K. X. Huang, G. F. Dai, C. Cao, R. J. Dong, *Bioorg. Med. Chem. Lett.* **2009**, *19*, 6637-6639.

[8] a) R. Liu, C. Gao, Y. G. Zhao, A. Wang, S. Lu, M. Wang, F. Maqbool, Q. Huang, *Bioresour. Technol.* **2012**, *123*, 86-91; b) B. Yu, E. Zhang, X. N. Sun, J. L.Ren, Y. Fang, B. L. Zhang, D. Q. Yu, H. M. Liu, *Steroids* **2013**, *78*, 494-499.

[9] a) B. L. Zhang, E. Zhang, L. P. Pang, L. X. Song, Y. F. Li, B. Yu, H.M. Liu, *Steroids* **2013**, *78*, 1200-1208; S. Gogoi, K. Shekarrao, A. Duarah, T. C. Bora, S. Gogoi, R. C. Boruah, *Steroids* **2012**, *77*, 1438-1445.

This article is protected by copyright. All rights reserved.

[10] a) M. Bu, B. B. Yang, L. M. Hu, *Curr. Med. Chem.* **2016**, *23*, 383-405; b) V. M. Dembitsky, T. A. Gloriozova, V. V. Poroikov, *Mini-Rev. Med. Chem.* **2007**, *7*, 571-589; c) Z. M. Zou, L. J. Li, D. Q. Yu, P. Z. Cong, *J. Asian Nat. Prod. Res.* **1999**, *2*, 55-61.

[11] a) T. Takei, M. Yoshida, M. Ohnishi-Kameyama, M. Kobori, *Biosci. Biotech. Bioch.* **2005**, *69*, 212-215; b) D. H. Kim, S. J. Jung, I. S. Chung, Y. H. Lee, D. K. Kim, S. H. Kim, B. M. Kwon, T. S. Jeong, M. H. Park, N. S. Seoung, N. I. Baek, *Arch. Pharm. Res.* **2005**, *28*, 541-545; c) S. T. Fang, X. Liu, N. N. Kong, S. J. Liu, C. H. Xia, *Nat. Prod. Res.* **2013**, *27*, 1965-1970.

[12] a) S. Zhao, G. Ye, G. Fu, J. X. Cheng, B. B. Yang, C. Peng, *Int. J. Oncol.* **2011**, *38*, 1319-1327; b) S. W. Kim, S. S. Park, T. J. Min, K. H. Yu, *B. Kor. Chem. Soc.* **1999**, *20*, 819-823; c) J. Han, E. J. Sohn, B. Kim, S. Kim, G. Won, S. Yoon, J. Lee, M. J. Kim, H. Lee, K. Chung, S. h. Kim, *Cancer Cell Int.* **2014**, *14*, 117-124; d) R. Zhu, R. Zheng, Y. Deng, Y. Chen, S. Zhang, *Phytomedicine* **2014**, *21*, 372-378; e) Y. H. Rhee, S. J. Jeong, H. J. Lee, H. J. Lee, W. Koh, J. H. Jung, S. H. Kim, K. Sung-Hoon, *BMC Cancer* **2012**, *12*, 28-38; f) M. Kobori, M. Yoshida, M. Ohnishi-Kameyama, H. Shinmoto, *Br. J. Pharmacol.* **2007**, *150*, 209-219.

[13] Q. P. Wu, Y. Z. Xie, Z. Deng, X. M. Li, W. Yang, C. W. Jiao, L. Fang, S. Z. Li, H. H. Pan, A. J. Yee, D. Y. Lee, C. Li, Z. Zhang, J. Guo, B. B. Yang, *PLoS One* **2012**, *7*, e44579.

[14] X. M. Li, Q. P. Wu, M. Bu, L. M. Hu, W. W. Du, C. W. Jiao, H. H. Pan, M. Sdiri, N. Wu, Y. Z. Xie and B. B. Yang, *Oncotarget* **2016**, *7*, 33948-33959.

[15] a) M. Klaper, T. Linker, *Chem. Eur. J.* **2015**, *21*, 8569-8577; b) B. W. Henderson, T. J. Dougherty, *Photochem. Photobio.* **1992**, *55*, 145-157.

[16] a) J. H. Park, S. V. Bhilare, S. W. Youn, *Org. Lett.* **2011**, *13*, 2228-2231; b) A. H. Banday, S. A. Shameem, B. D. Gupta, H. M. S. Kumar, *Steroids* **2010**, *75*, 801-804.

[17] X. Zhang, Q. Ba, Z. Gu, D. Guo, Y. Zhou, Y. Xu, H. Wang, D. Ye, H. Liu, *Chem. Eur. J.* **2015**, *21*, 17415-17421.

[18] a) M. S. Aw, M. Kurian, D. Losic, *Chem. Eur. J.* **2013**, *19*, 12586-12601; b)M. Kodiha, Y. M. Wang, E. Hutter, D. Maysinger, U. Stochaj, *Theranostics* **2015**, *5*, 357-370.

[19] a) T. Sun, X. Guan, M. Zheng, X. Jing, Z. Xie, *ACS Med. Chem. Lett.* **2015**, *6*, 430-433; b) R. Kumar, J. Han, H. J. Lim, W. X. Ren, J. Y. Lim, J. H. Kim, J. S. Kim, *J. Am. Chem. Soc.* **2014**, *136*, 17836-17843.

[20] a) S. Wu, Q. Cao, X. Wang, K. Cheng, Z. Cheng, *Chem. Commun.* **2014**, *50*, 8919-8922; b) D. Guo, T. Chen, D. Ye, J. Xu, H. Jiang, K. Chen, H. Wang, H. Liu, *Org. Lett.* **2011**, *13*, 2884-2887.

[21] M. A. Ponce, J. A. Ramirez, L. R. Galagovsky, E. G. Gros, R. Erra-Balsells, *Photoch. Photobio. Sci.* **2002**, *1*, 749-756.

[22] D. Flesch, M. Gabler,; A. Lill, R. C. Gomez, R. Steri, G. Schneider, H. Stark, M. Schubert-Zsilavecz, D. Merk, *Bioorg. Med. Chem.* **2015**, *23*, 3490-3498.

WILEY-VCH Accepted Manuscript

This article is protected by copyright. All rights reserved.

FULL PAPER

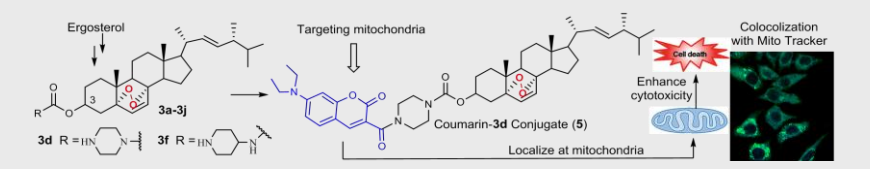

Small changes, big difference! Through structural changes to synthesized a series of 5α,8α-ergosterol peroxide 3-carbamate derivatives (**3a**-**3j**). Compound **3d**, **3f** and their hydrochloride exhibited significant *in vitro* anti-proliferative activity against the tested tumor cell lines. Fluorescence mitochondria-targeting conjugate **5** was obtained by linking coumarin-3-carboximide with **3d**. The probe localized in mitochondria, leading to enhanced anticancer activity over the parent structure.

Ming Bu,[a] Tingting Cao,[a] Hongxia Li,[a] Mingzhou Guo,[c] Burton B. Yang,[d] Chengchu Zeng[a] and Liming Hu[a,b]*

Page No. – Page No.

Synthesis of 5α,8α-ergosterol peroxide 3-carbamate derivatives and fluorescent mitochondria-targeting conjugate for enhanced anticancer activities

WILEY-VCH Accepted Manuscript

This article is protected by copyright. All rights reserved.